Marine *Synechococcus* picocyanobacteria: Light utilization across latitudes

Christophe Six[a,1], Morgane Ratin[a], Dominique Marie[a], and Erwan Corre[b]

[a]Centre National de la Recherche Scientifique, Sorbonne Université, UMR 7144, Adaptation et Diversité en Milieu Marin, group Ecology of Marine Plankton, Station Biologique de Roscoff, 29680 Roscoff, France; and [b]Department Analysis and Bioinformatics for Marine Science, Fédération de Recherche 2424, 29680 Roscoff, France

Edited by Susan S. Golden, University of California San Diego, La Jolla, CA, and approved August 3, 2021 (received for review June 24, 2021)

The most ubiquitous cyanobacteria, *Synechococcus*, have colonized different marine thermal niches through the evolutionary specialization of lineages adapted to different ranges of temperature seawater. We used the strains of *Synechococcus* temperature ecotypes to study how light utilization has evolved in the function of temperature. The tropical *Synechococcus* (clade II) was unable to grow under 16 °C but, at temperatures >25 °C, induced very high growth rates that relied on a strong synthesis of the components of the photosynthetic machinery, leading to a large increase in photosystem cross-section and electron flux. By contrast, the *Synechococcus* adapted to subpolar habitats (clade I) grew more slowly but was able to cope with temperatures <10 °C. We show that growth at such temperatures was accompanied by a large increase of the photoprotection capacities using the orange carotenoid protein (OCP). Metagenomic analyzes revealed that *Synechococcus* natural communities show the highest prevalence of the *ocp* genes in low-temperature niches, whereas most tropical clade II *Synechococcus* have lost the gene. Moreover, bioinformatic analyzes suggested that the OCP variants of the two cold-adapted *Synechococcus* clades I and IV have undergone evolutionary convergence through the adaptation of the molecular flexibility. Our study points to an important role of temperature in the evolution of the OCP. We, furthermore, discuss the implications of the different metabolic cost of these physiological strategies on the competitiveness of *Synechococcus* in a warming ocean. This study can help improve the current hypotheses and models aimed at predicting the changes in ocean carbon fluxes in response to global warming.

Synechococcus | temperature | cyanobacteria | orange carotenoid protein | photosynthesis

The world ocean plays a central role in the climate regulation of the planet, in particular through the metabolic activity of the huge diversity of microorganisms it shelters. Among these, oxygenic phototrophs (i.e., phytoplankton) are responsible for major gas exchanges and carbon fluxes at global scale. Marine *Synechococcus*, the most widespread cyanobacterial genus on Earth, are extremely abundant phytoplanktonic cells thought to be responsible for a large part of the global net oceanic primary production (1). The quasi ubiquity of these picocyanobacteria relies on their current microdiversity, which results from the broad diversification of their radiation, including about 15 clades and 28 subclades [subcluster 5.1; (2, 3)]. Global phylogeographical studies have shown that the most prevalent *Synechococcus* lineages occupy distinct ecological niches notably defined on abiotic factors, such as nutrients, light quality, and temperature (see e.g., refs. 3–7). In particular, members of clades I and IV have been shown to dominate in cold, high-latitude waters, while clades II and III thrive in the warm intertropical areas. These *Synechococcus* ecotypes have different thermal preferenda that reflect their respective thermal niches (8, 9), showing that temperature has greatly influenced the diversification of these organisms because it constitutes a major ecological constraint on cell physiology.

Photosynthesis is considered to be among the most temperature-sensitive cell processes of phototrophic organisms. Only a few studies have highlighted how, during their evolution, temperature has shaped the genomes of marine *Synechococcus*, but most of the studied processes are linked to photosynthesis. For instance, the composition of the photosynthetic membranes, the thylakoids, is highly thermoregulated through distinct physiological strategies set up by the different *Synechococcus* temperature ecotypes (10, 11). In addition, amino acid substitutions in key photosynthetic proteins have led to the diversification of protein variants that have allowed the thermoadaptation of the light-harvesting process (12).

The major light-harvesting system of *Synechococcus* is a giant, water-soluble pigment–protein complex called the phycobilisome, which funnels light energy to the photosystem II (PSII) reaction center carrying out the photosynthetic primary charge separation. The phycobilisome is composed of a central core surrounded by rods of phycobiliproteins assigned to distinct classes. While the core is always made of allophycocyanin, the rods are composed of phycocyanin and, in most marine *Synechococcus*, of two types of phycoerythrins (PE), PEI and PEII, displaying different combinations of phycobilin chromophores, depending on the strain (13–15). The phycobilisome thus constitutes the main entrance gate of light energy into the cyanobacterial cell. However, when light is excessive (i.e., when the rate of PSII charge separation outpaces the rate of electron utilization), the phycobilisome components are usually down-regulated in order to decrease PSII light absorption cross-section, thereby limiting the production of

Significance

Phytoplankton drives most of the carbon pumping of the world ocean through the photosynthesis process. We show how *Synechococcus* picocyanobacteria, a very abundant marine phytoplankton, have adapted the light utilization process to colonize different thermal niches. At high temperature, tropical *Synechococcus* induce strong synthesis of most photosynthetic complexes and can thus considerably increase growth. By contrast, subpolar *Synechococcus* grow more slowly but are capable of surviving at low temperature. To do so, they notably use the photoprotective orange carotenoid protein, and we show that temperature has been a major factor in the molecular evolution of this protein in the oceans. Our study can allow the improving of current models predicting the changes in carbon fluxes in a warming ocean.

Author contributions: C.S. designed research; C.S., M.R., D.M., and E.C. performed research; C.S., M.R., and E.C. analyzed data; and C.S. wrote the paper.

The authors declare no competing interest.

This article is a PNAS Direct Submission.

[1]To whom correspondence may be addressed. Email: six@sb-roscoff.fr.

This article contains supporting information online at https://www.pnas.org/lookup/suppl/doi:10.1073/pnas.2111300118/-/DCSupplemental.

Published September 13, 2021.

reactive oxygen species that can induce a lethal oxidative stress situation (16–18).

Another essential mechanism for the regulation of light utilization is the dissipation of excess light into heat. In cyanobacteria, the best-studied photoprotective process of this type relies on the activity of a three-gene operon that encodes and regulates the activity of a water-soluble, keto–carotenoid binding protein named the orange carotenoid protein (OCP). This protein, discovered decades ago (19) and characterized much later (20), undergoes a photocycle whose details have been extensively studied in freshwater cyanobacteria (21–23). Upon activation by blue-green light, the carotenoid is translocated between the two globular domains, and the color of the protein turns to red. The red protein binds to the phycobilisome core, intercepting light energy and inducing its thermal dissipation. OCP activity is measurable as nonphotochemical quenching of chlorophyll fluorescence (NPQ), which is associated to the decrease of the energy reaching reaction centers. When light is no more excessive, the fluorescence recovery protein, encoded in the OCP operon, induces the OCP detachment from the allophycocyanin core, and the dissipation stops. OCP genes are present in many phycobilisome-containing cyanobacteria genomes and three paralogous families of OCP have been described. The largest and most diverse group is the OCP1 family, which includes all the OCPs of marine *Synechococcus*. To date, OCP proteins have been well studied in freshwater cyanobacterial models, but the marine OCPs, which are definitively very divergent from their freshwater counterparts (24), have never been studied.

We used a multiscale approach, including biophysics, biochemistry, genomics, and ocean metagenomics, to better understand how light utilization has evolved in marine *Synechococcus* across latitudes. The capacity of tuning phycobilisome light absorption versus OCP light dissipation was compared in several *Synechococcus* temperature ecotypes. This led us to study the different marine OCP variants and their global distribution in the world ocean. Our study unveils the major influence of temperature on the evolution of this protein in the oceans and sheds light on the *Synechococcus* physiological strategies involved in the response to the current global changes.

Results and Discussion

Differential Regulation of Growth and Light-Harvesting Capacities. *Synechococcus* strains M16.1 (subcluster 5.1, clade II) and MVIR-18-1 (subcluster 5.1, clade I; Fig. 1 *A* and *B*) have colonized contrasted thermal niches of the world ocean (3, 4, 6). M16.1 was isolated in the Gulf of Mexico, where the waters reach 30 °C, whereas MVIR-18-1 was isolated in the subpolar waters of the Norway sea, where the temperature is as low as 6 °C in winter. The cold-adapted ecotype MVIR-18-1, which displays higher-cell biovolume (Fig. 1*C*), showed a moderate increase in cell size with increasing growth temperature, whereas the warm-adapted ecotype M16.1 was smaller but induced a biovolume doubling, then reaching biovolume values similar to the cold-adapted strain. This cell size difference supports the so-called "temperature-size rule," which states that there is a negative relationship between ambient temperature and organism size (25). However, these results show that the cell size of the smallest organisms can increase with growth temperature, and our study suggests that this is probably linked to the regulation of light utilization and growth rate. The growth capacities of these two *Synechococcus* in our experimental conditions supported previous studies showing that they display distinct thermal preferenda [Fig. 1*D*; (8)]. The tropical strain M16.1 showed optimal growth at 33 °C, whereas the optimal temperature was about 10 °C lower for the subpolar one. The thermal limits for growth also differed drastically, with M16.1 growing from 18 to 32 °C, whereas MVIR-18-1 was not able to grow above 26 °C but maintained measurable growth below 9 °C. These two isolates,

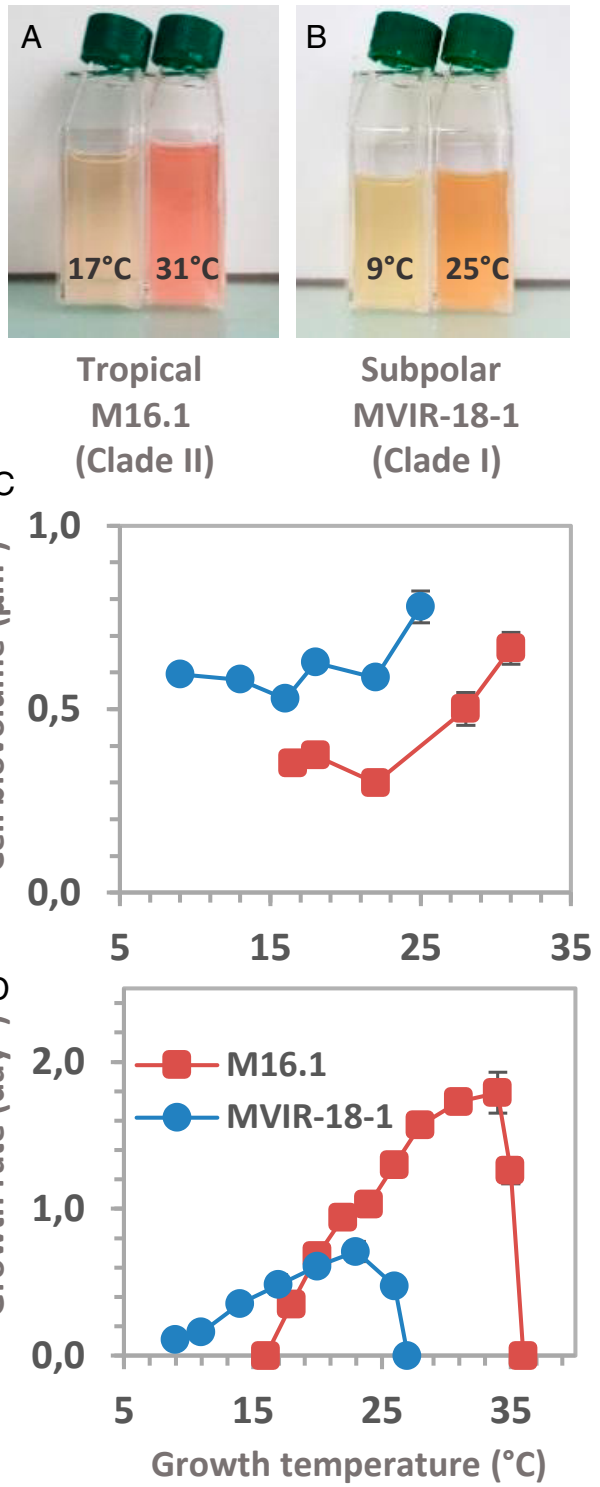

Fig. 1. Culture flasks of *Synechococcus* picocyanobacteria strains M16.1 (*A*) (tropical; clade II) and MVIR-18-1 (*B*) (subpolar; clade I) grown at their thermal growth limits (cell density between 4 and 6 10^7 cells · mL^{-1}). Variations of cell biovolume (*C*) and growth rate (*D*) in *Synechococcus* spp. M16.1 (red) and MVIR-18-1 (blue), function of growth temperature, as measured by flow cytometry.

which are among the most contrasted marine *Synechococcus* thermotypes studied so far, also differed in the growth rate values they were capable of inducing. The subpolar strain never reached growth rates higher than 0.7. The tropical strain triggered very

rapid growth, starting from a curve shoulder at 25 °C, which was the temperature at which the subpolar strain reached maximal growth before declining. These growth responses have previously been observed in other marine *Synechococcus* strains (8). This suggests that, at this temperature and in contrast to the clade I subpolar strain, the clade II tropical ecotype induced specific physiological mechanisms, allowing considerable growth acceleration.

In order to better understand the mechanisms lying behind these different growth responses to temperature, we studied the relation between thermal acclimation and the regulation of photosynthesis, the major energetic process in these organisms. Pulse amplitude modulation (PAM) fluorometry analyses unambiguously showed that green (540 nm) and cyan (480 nm) lights are by far the most utilized wavelengths by these cyanobacteria, in agreement with their phycoerythrobilin-rich pigment type 3a (14), and we therefore focused our work on these wavelengths. Analysis of electron flow through PSII (ETRII) versus irradiance curves revealed that the PSII saturation irradiance E_K of the tropical strain drastically decreased at high temperature, along with an increase of the PSII efficiency α (Fig. 2*A* and *SI Appendix*, Figs. S1 and S2). In the clade I subpolar strain, these parameters varied much less. This shows that the clade II tropical strain was capable of a very flexible photophysiological response, inducing the efficient exploitation of the photon flux at high temperature. This was associated to an increase in chlorophyll *a* (chl *a*) and β-carotene cell contents in both strains, which was much more pronounced in the tropical strain (Fig. 2 *B–D*). As these two pigments are mostly located in the thylakoidal membranes, in the photosystem reaction centers, this suggests that acclimation to high temperature in the tropical strain induced a marked synthesis of additional thylakoid lamellas and/or photosystems, which allowed a strong increase of the rate of photosynthetic electron transport per cell. This synthesis of additional thylakoid membranes is likely associated to the marked increase in cell biovolume (Fig. 1*C*). Comparison of the cell content in PSII and PSI, using anti-PsbD and anti-PsaC antibodies (Fig. 2 *E* and *F* and *SI Appendix*, Fig. S3), respectively, confirmed an enhanced photosystem biosynthesis in response to increasing growth temperature. The tropical strain M16.1, however, reached higher-PSII cell contents, while the PSI cell content variations were similar between the two strains over their thermal growth range. When the data were expressed in biovolume units (*SI Appendix*, Fig. S3), it could be observed that both strains have identical PSI content per cubic micrometer cell with a linear, temperature-induced increase. However, it seems that the subpolar strain could not increase anymore with the PSII content per cubic micrometer cell at temperatures higher than 22 °C. Together, with the increase in the β-carotene: chl *a* ratio in M16.1 (*SI Appendix*, Fig. S4), this suggests an increase of the number of PSII relative to PSI in the tropical strain in response to increasing growth temperature, likely leading to higher-transthylakoidal pH gradient and consequent higher-ATP production (11). It will be interesting in future research to study the possible molecular differences (differential thermostability, protection by other proteins, occurrence of thermostable protein isoforms, etc.) in the photosynthetic complexes of these temperature ecotypes, in order to better understand the physiological factors that prevent/allow growth at high temperature (12).

We analyzed the light-harvesting capacities of both strains grown over their thermal preferenda. In response to increasing temperature, the PE cell content increased much more in the clade II tropical strain than in the clade I subpolar one, as measured by flow cytometry, spectrofluorimetry (Fig. 2*G* and *SI Appendix*, Fig. S5*A*), and direct quantification of the β-subunit of the major light-harvesting proteins, PEI and PEII (Fig. 2*H* and *SI Appendix*, Fig. S3). The tropical strain reached PE cell contents twice higher than the subpolar strain, thereby giving a bright pink color to the M16.1 cultures. This shows that, in response to increasing temperature, the tropical strain drastically increased its light absorption capacities by inducing strong synthesis of PE and most probably of entire phycobilisomes, as supported by the concomitant increase of the whole-cell phycocyanin fluorescence (*SI Appendix*, Fig. S5*B*). Consequently, while the molar PE to PSII ratio of the subpolar strain remained fairly stable at ∼36 hexamers per PSII, the tropical strain increased it from 20 to 43 PE hexamers per PSII (*SI Appendix*, Fig. S6). This resulted in a strong increase of the PSII absorption cross-section σ(II) at 540 and 480 nm for the tropical strain at high temperature [Fig. 2*I* and *SI Appendix*, Fig. S7; (26)].

To estimate whether this difference of response to growth temperature was specific to these two strains or a more general physiological strategy of marine *Synechococcus* cyanobacteria, we investigated the capacity to modulate σ(II) in the blue-green region in seven other phycoerythrobilin-rich *Synechococcus* strains. Among the strains we tested, those belonging to the warm-adapted clades II and V all deployed the largest effective photosynthetic antennae when grown at high-growth temperature, with σ(II) being approximately threefold higher than at low temperature (Fig. 2*K* and *SI Appendix*, Fig. S8). By contrast, the maximal σ(II) was significantly lower among the cold-adapted strains from clades I and IV. While clade I strains and the clade IV strain BL107 showed low or no capacities to increase σ(II) in response to high temperature, the cold, temperate clade IV strain MVIR-16-1 significantly increased σ(II) at high-growth temperature. Overall, these results suggest that warm-adapted strains from clade II and V can induce very large photon absorption in response to high temperature, whereas cold-adapted strains have smaller photosynthetic antennae with strain-specific regulation capacities. There is little doubt that the ability of clade II tropical *Synechococcus* to markedly increase σ(II) and the thylakoidal components of the photosynthetic apparatus is directly linked with the capacity to considerably accelerate growth rate in response to increased temperature (8), whereas the clade I subpolar strains are unable of it.

The quantification of the ribulose-1,5-bisphosphate carboxylase oxygenase (RuBisCO) enzyme, catalyzing photosynthetic carbon fixation, revealed further differences between the two strains. The tropical strain increased the RuBisCO cell content, following its increase in biovolume, so that the RuBisCO content per cubic micrometer cell remained stable over the thermal growth range (Fig. 2*J* and *SI Appendix*, Fig. S3). The subpolar strain showed similar RuBisCO content to the tropical one between 16 and 25 °C but increased the mean RuBisCO content for temperatures lower than 16 °C. Like for any enzyme, RuBisCO activity cannot be estimated using the sole protein content. It is well known that RubisCO needs to be activated by the regulatory protein RuBisCO Activase, which has been shown to be temperature sensitive (27, 28). In many plants, under cold stress, the RuBisCO content is up-regulated in order to compensate for the decline of the carboxylase turnover rate (29) often induced by the RuBisCO Activase activity drop. Our results thus suggest that, in the subpolar strain, the carboxylase turnover rate of the RuBisCO is significantly affected under 16 °C. As the subpolar niches are the limit of the global latitudinal distribution of marine *Synechococcus*, it is possible that the specific, molecular characteristics of the RuBisCO system in these cyanobacteria hinder the colonization of the colder polar niches.

Xanthophylls and Temperature-Induced Photoprotection. Marine *Synechococcus* have a simple carotenoid composition based on the CrtL-b cyclase pathway (30). From β-carotene, a few xanthophylls can be synthetized, several of which have never been identified (*SI Appendix*, Fig. S9). Upon growth temperature changes, the conversion of β-carotene into β-cryptoxanthin, catalyzed by the CrtR enzyme, did not seemingly change in the two strains, since the cell content in the two carotenoids increased similarly with increasing temperature (Figs. 2*D* and 3*A* and *SI Appendix*, Fig. S10*A*).

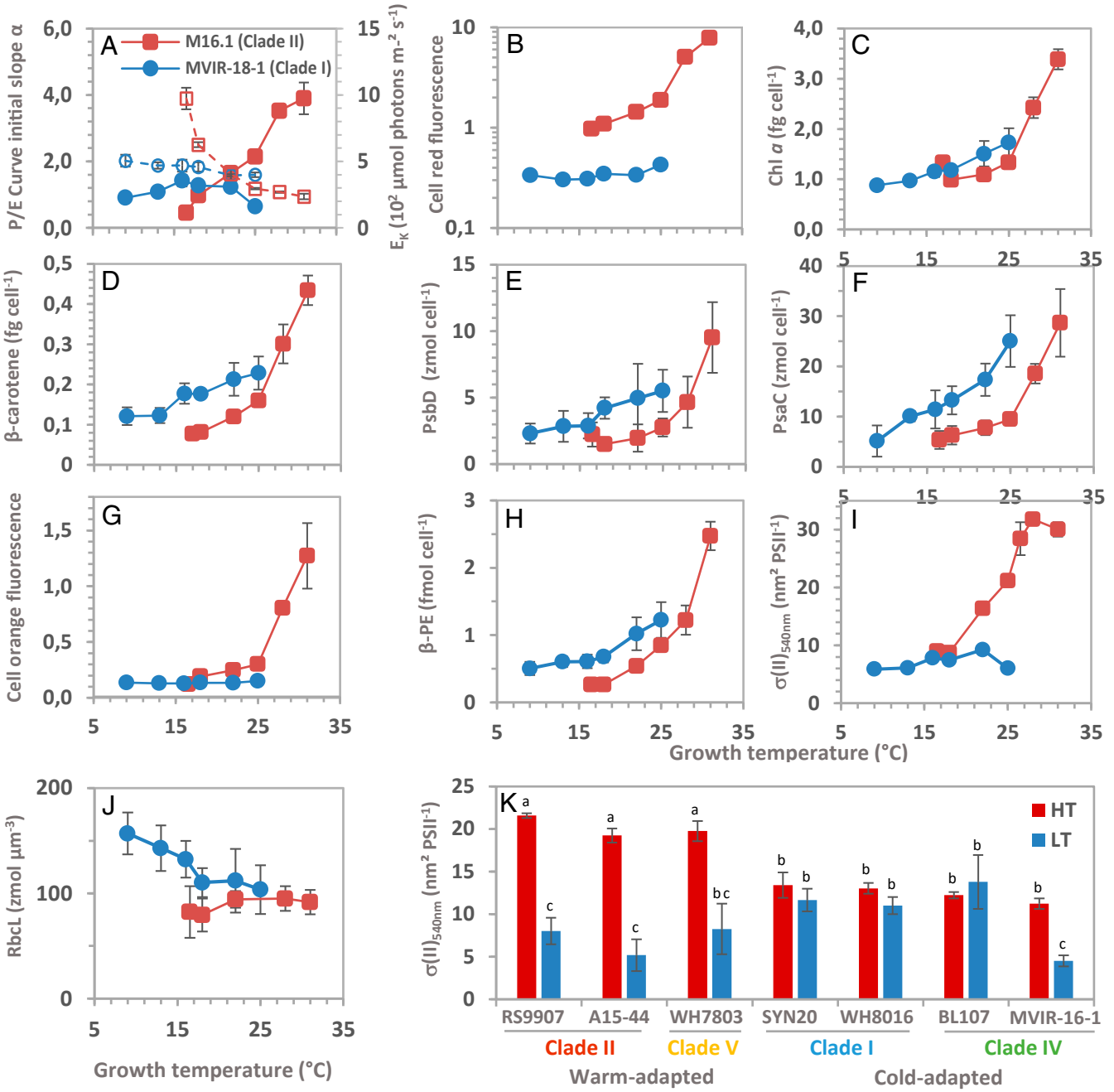

Fig. 2. Variations of photophysiological parameters in the tropical M16.1 (clade II; red) and subpolar MVIR-18-1 (clade I; blue) *Synechococcus* strains, function of growth temperature. (*A*) Initial slope (α) of the electron transport versus 540-nm irradiance (P/E) curve (filled symbols), reflecting the photon-dependent efficiency of PSII in low irradiance and saturation 540 nm irradiance (E_K) of the same curve (empty symbols), indicating the green photon flux necessary to saturate PSII activity. (*B*) Chlorophyll *a* cellular fluorescence emitted at 680 nm, as measured by flow cytometry. (*C*) Chlorophyll *a* cell content, as measured by high-pressure liquid chromatography. (*D*) β-carotene cell content, as measured by high-pressure liquid chromatography. (*E*) Cell content in PsbD (D2), a major core protein of PSII, as measured by quantitative immunoblotting. (*F*) Cell content in PsaC, a protein of PS I, as measured by quantitative immunoblotting. (*G*) PE cellular fluorescence emitted at 525 nm, as measured by flow cytometry. (*H*) Cell content in β-PE subunits (MpeB and CpeB), as measured by quantitative in-gel fluorescence. (*I*) PSII absorption cross-section at 540 nm, reflecting the effective size of the photosynthetic antenna. (*J*) Cell biovolume content in RbcL, the large subunit of the RuBisCO, as measured by quantitative immunoblotting. (*K*) Variations of the PSII absorption cross-section at 540 nm in different temperature ecotypes of marine *Synechococcus* grown near their growth thermal limits (HT, high growth temperature; LT, low growth temperature). Small error bars may be hidden by the symbols. Statistics tests (Kruskal–Wallis test, $df = 3$ and P value < 0.05) are represented with the letter notation.

β-cryptoxanthin can be converted using the same enzyme into zeaxanthin, by far the most accumulated xanthophyll in all marine *Synechococcus*. Whereas in the subpolar ecotype the zeaxanthin cell content did not vary with growth temperature, it increased in the tropical strain starting from 25 °C, similarly to the thylakoidal photosynthetic complexes (Fig. 3*B*). This led to weaker variations of the zeaxanthin to β-cryptoxanthin ratio in the MVIR-18-1 than in M16.1 (*SI Appendix*, Fig. S10*B*), while the global zeaxanthin to chl *a* ratio decreased in the two strains following a similar rate (*SI Appendix*, Fig. S10*C*). Although the function of zeaxanthin remains

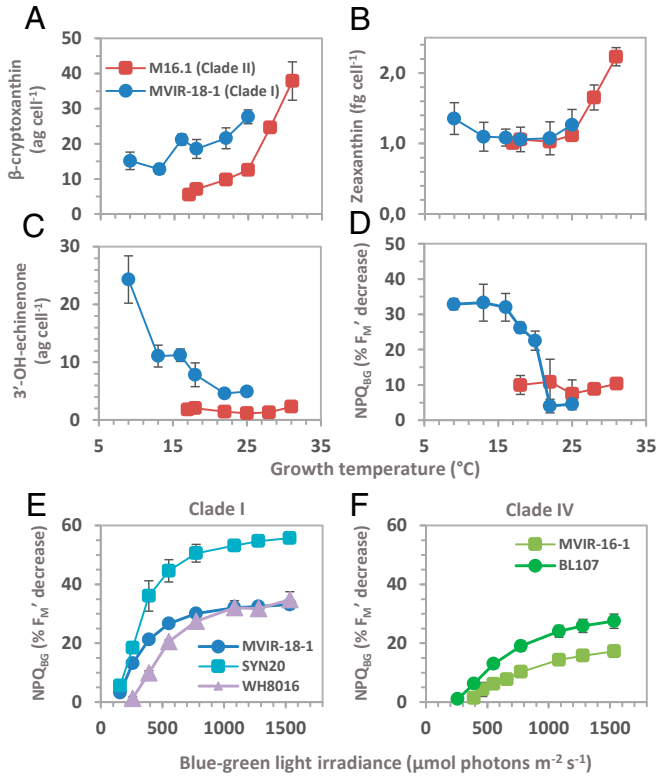

Fig. 3. Variations in xanthophyll cell content and NPQ_{BG} function of growth temperature. Cell content in β-cryptoxanthin (*A*), zeaxanthin (*B*), and 3′-hydroxyechinenone (*C*). (*D*) Variations in NPQ_{BG}, as measured by pulse amplitude modulation fluorometry, expressed in the percentage of decrease of the F_{M}' level. Irradiance (480 nm) response curve of NPQ_{BG} in *Synechococcus* strains belonging to the subpolar clade I (*E*, blue and purple) and the cold temperate clade IV (*F*, green).

unclear in marine *Synechococcus*, this suggests that it is localized within the thylakoids.

The most interesting observation was that a part of the β-cryptoxanthin was converted in 3′-hydroxyechinenone in the clade I subpolar strain at low-growth temperature, whereas this xanthophyll kept stable at low-cell content in the clade II tropical strain (Fig. 3*C*). This reaction is catalyzed by the CrtW ketolase enzyme (*SI Appendix*, Fig. S11), whose gene is part of the small OCP operon. This cyanobacterial protein generally binds 3′-hydroxyechinenone and, upon blue-green light activation, interacts with the allophycocyanin phycobilisome core to dissipate light energy before it reaches the photosystem reaction center (31). This photoprotective process, which limits photosynthetic electron jamming and the subsequent induction of oxidative stress, is measurable as the nonphotochemical quenching of chl *a* fluorescence. In order to determine whether the increase in 3′-hydroxyechinenone was associated to the induction of OCP-mediated photoprotection, we studied the capacity to induce nonphotochemical quenching of PSII fluorescence under blue-green light (NPQ_{BG}), using inactinic, phycobilisome-absorbed light (540 nm) and actinic, OCP-absorbed light (480 nm) to monitor the energy transfer from the phycobilisome to the PSII (22). The results unambiguously showed that the subpolar *Synechococcus* sp. MVIR-18-1 has large NPQ_{BG} induction capacities under low-growth temperature (Fig. 3*D*). After the relaxation of the state transition process under low light, high light at 480 nm provoked a rapid drop of both the basal (F_0) and maximal (F_M') PSII fluorescence levels, which was reversible under low light (*SI Appendix*, Fig. S12). We were able to induce NPQ_{BG} only using the 440- and 480-nm wavelengths available on our fluorometer. By contrast, the tropical strain was able to induce only low and variable levels of NPQ_{BG}, which did not seem to be related to growth temperature. Considering that the OCP binds a single 3′-hydroxyechinenone molecule and using our quantitative phycobiliprotein data, we calculated that the number of OCP per allophycocyanin increased in the subpolar strain from 0.35 at 25 °C to 3.4 at 9 °C, which are values comparable to those reported for *Synechocystis* sp. PCC 6803 (32).

Boulay and coworkers reported NPQ_{BG} induction in four marine *Synechococcus* strains grown at 22 °C, which were all isolated from warm environments (33). This induction was, however, rather low, similarly to what we observed in the clade II tropical strain *Synechococcus* sp. M16.1. In addition, large-scale, proteomic and transcriptomic studies reported the accumulation of OCP transcripts and proteins in response to low temperature in three marine *Synechococcus* strains (9, 34). To provide insights on whether this photophysiological response is thermotype specific, we investigated the capacity of other *Synechococcus* strains to induce NPQ_{BG} in response to low-growth temperature. We grew the model strain WH7803 (clade V) and five strains (RS9907, A15-44, RS9915, WH8102, and BOUM118) belonging to the warm-adapted clades II and III at temperatures close to the limits of their growth thermal range. Similarly, to what we describe in more detail for the clade II strain M16.1 (Fig. 3*D* and *SI Appendix*, Fig. S12), all strains belonging to clades II and III showed no or limited NPQ_{BG} induction. We also grew five other *Synechococcus* strains belonging to the two cold-adapted clades I and IV close to the limits of their thermal preferendum. All of them induced more or less large NPQ_{BG} in response to low-growth temperature only. This suggests that the capacity to induce large NPQ_{BG} might be a feature of *Synechococcus* strains adapted to cold environments. In such thermal niches, photosynthetic organisms may undergo a slowing down of major metabolic processes, like the maintenance of the PSII complexes through the PSII repair cycle, which is partly based on the excision and replacement of nonfunctional D1 proteins from the PSII core (35). At low temperature, this constitutes a strongly limiting step for efficient PSII repair, as exemplified in marine diatoms (36, 37) and the green picoalga *Micromonas polaris* (38). Thus, the capacity to induce significant NPQ, protecting the cell from PSII-induced oxidative stress, may therefore be critical to maintain significant growth at low temperature.

To further characterize and compare the response of the two clades (I and IV) of cold-adapted strains, we built irradiance response curves of NPQ_{BG} in cultures all acclimated to 14 °C (Fig. 3 *E* and *F*). Clade I strains started inducing measurable NPQ_{BG} at 150 to 200 µmol · photons · m^{-2} · s^{-1} blue-green light, and the curves saturated at irradiances higher than ~1,000 µmol · photons · m^{-2} · s^{-1}. The maximal NPQ_{BG} levels depended on the strain and were comprised between the 30 and 55% decrease of the maximal F_M' level. These characteristics are comparable to previous observations in freshwater cyanobacteria strains (33, 39, 40). Compared to clade I strains, the clade IV strains started inducing NPQ_{BG} at higher irradiances and did not show full saturation in our experimental conditions. Comparing modeled NPQ_{BG} saturation irradiance values confirmed that clade IV strains saturated NPQ_{BG} at significantly higher photon fluxes (*SI Appendix*, Fig. S13). These differences of NPQ_{BG} induction between strains of the two cold-adapted clades were also visible on Ln-transformed curves, which showed that subpolar clade I strains are able to induce more NPQ_{BG} per incident photon than the cold, temperate clade IV strains (*SI Appendix*, Fig. S13). These differences in OCP activity between the two cold-adapted clades are possibly related to their different, though overlapping, thermal distribution, since clade IV strains inhabit slightly warmer waters than clade I.

The capacity of cold-adapted strains to induce strong light dissipation at low temperature, and the differences among the strains/clades can originate from a strong activation of the OCP operon, leading to a high cellular ratio of active OCP to phycobilisome, and/or from the presence of OCP variants displaying different efficiencies. Further research using purified marine OCPs and genetic transformation techniques is necessary to answer these questions.

Molecular Characteristics of OCP Variants. Muzzopappa and coworkers showed that marine OCPs are phylogenetically very distant from their freshwater counterparts (24), raising questions about the selective pressures at work behind this differential evolution. Using metagenomic data and recently published *Synechococcus* genomes (41), we built a database of 70 complete sequences of marine *Synechococcus* OCPs. First observations revealed that among all the known marine *Synechococcus* clades, only some of them include genomes containing the OCP operon, namely clades I, II, III, IV, V, VI, VIII, WPC1, and subcluster 5.3. The recently discovered phycobilisome-containing *Procchlorococcus* genomes do not contain the OCP operon (42). Studying the phylogenetic relationships among these protein sequences showed that the OCPs of the clade I subpolar *Synechococcus* are the most distant proteins from all other oceanic OCPs (Fig. 4*A*). Interestingly, the OCPs of clade IV *Synechococcus*, the other cold-adapted clade inhabiting cold, temperate waters, form a sister group to the clade I subpolar OCPs. This was quite unexpected, because the two cold-adapted clades I and IV have been shown to belong to two distinct taxonomic subgroups (5.1A and 5.1B) in the topology of the core phylogenies (see e.g., refs. 2, 4, and 41). Overall, these observations suggest that *ocp* genes from cold regions of the oceans have evolved differently from the others. Moreover, the fact that OCPs from *Synechococcus* clades I and IV, distant in the core phylogenies, show relatively high sequence similarity suggests an evolutionary convergence under cold temperature selection pressure and/or that the proteins originate from a relatively recent horizontal transfer of genes between the two cold-adapted clades.

The structure of freshwater OCPs has been studied in detail (21), and most of the amino acids for which important structural functions have been evidenced are conserved in marine OCPs, with some minor substitution (39, 43; *SI Appendix*). This suggests that the OCP photocycle mechanism is well conserved in marine *Synechococcus*. However, a global bioinformatic analysis of the properties of the different marine OCPs gave insights on the evolution of this protein in the oceans. First, there is an apparent relationship between the molecular weight of the apoprotein and the thermal niche of the strains. For an equal number of amino acids, subpolar OCPs are ∼500 Da lighter than the tropical ones, while temperate OCPs show intermediate molecular weights (Fig. 4*B*; Kruskal–Wallis test: $df = 3$ and P value < 0.05). In addition, clade I OCPs are enriched in glycine, depleted in glutamine and leucine (Fig. 4*C* and *SI Appendix*, Fig. S14), and display a lower-aliphatic index, a proxy for the relative volume occupied by aliphatic side chains (Fig. 4*D*). OCPs from both cold-adapted clades I and IV have a higher content in serine. These differences are well known to constitute molecular adaptations to different thermal niches (44–46). For instance, a high content in the smallest amino acid glycine and a low content in hydrophobic amino acids, increase the molecular flexibility of a given protein variant. In cold habitats, where low temperature rigidifies macromolecules, the regulation of this physical parameter is essential in order to maintain the efficient activity of proteins. These conserved modifications in orthologous proteins from organisms that have evolved under different thermal environments, maintain optimal physiology and provide higher fitness in a given ecological niche.

We analyzed the predicted molecular flexibility of the OCP variants (Fig. 4*E*). The global pattern of chain flexibility was similar among OCPs, but specific regions of the cold-adapted OCPs showed clear differences. These proteins displayed higher flexibility in regions of the N-terminal domain, especially between residues 68 and 85, notably due to substitutions consisting in the replacement of an aspartate and a threonine at position 76 and 79, respectively, by serine residues. OCPs from the cold, temperate *Synechococcus* clade IV also showed higher-flexibility regions in the N- and C-terminal domains, which they share with the subpolar OCPs, in particular in the regions of residues 205 to 210 in which, notably, a serine replaces an alanine. The linker region between the two domains of the clade I subpolar OCPs displays the most different pattern of predicted flexibility. The superimposition of structural homology models of the OCP of the subpolar strain MVIR-18-1 and of the tropical strain M16.1 also clearly evidences a different conformation of the linker region (*SI Appendix*, Fig. S15). During the activation by blue-green light, the two domains of the OCP, which are bound by this linker, are separated in order to allow fixation on the phycobilisome (21). It is likely that this drastic conformation change of the protein, requiring high-molecular flexibility of the linker region, can be impacted by low temperature. The observed modification of the flexibility of the linker of subpolar OCPs likely allows maintaining the efficient activation of the OCP in the low-temperature conditions prevailing in subpolar niches.

Temperature-Guided Evolution of OCPs in the Marine *Synechococcus* Radiation. The inspection of 50 genomes of marine *Synechococcus* [Cyanorak database (47)] showed that, among representative strains of the four clades dominating the natural communities, the ecotypes adapted to cold and temperate environments (clades I, IV, and III) all have the OCP operon, whereas it is absent in ∼60% of the tropical clade II strains. This might be linked with the fact that several clade II *Synechococcus* have been shown to possess significantly smaller genomes (5), a characteristic that recalls the highly streamlined genomes of surface *Prochlorococcus*. The absence of the OCP operon in many clade II tropical *Synechococcus* suggests that, in the oceans, the OCP activity might not be essential to marine *Synechococcus* inhabiting warm and stable thermal environments.

Further examination showed that the genomic context of the OCP operon in marine *Synechococcus* genomes is relatively conserved in clades I, III, and IV. However, in the genomes of the few clade II strains that have the OCP operon, the latter is surrounded by more variable genes, including unique and clade II–specific genes. Furthermore, in most of these genomes, the OCP operon is contiguous to two genes involved in viral attacks and DNA insertion. The former (CK_00002022) encodes a protein harboring a PIN domain, induced during cyanophages infection (48). The second gene (CK_00033379) encodes a protein, showing similarity to DNA-processing chain A proteins, DprA. In many bacteria, these proteins are required for natural chromosomal and plasmid transformation, and they have been proposed as new members of the recombination–mediator protein family, allowing natural bacterial transformation (49). Like the recently described tycheposons (50), these genes might constitute a hallmark of horizontal gene transfer. It is worth noting that, in the other clades, these two genes are present but are associated with other gene clusters. These observations suggest that the OCP operon, in the few clade II strains that have it, could originate from a recent integration event, possibly following a more ancient, quasiintegral loss of the operon in the tropical clade II. The weak or absent response of the OCPs of warm-adapted *Synechococcus* to high light in low-temperature conditions may suggest that the OCP serves other types of acclimation responses in these cyanobacteria. For instance, although it has been less studied than the NPQ_{BG} mechanism, OCPs are known to be excellent quenchers of singlet oxygen (51). It is also possible that the OCP NPQ_{BG} in warm *Synechococcus* thermotypes is induced upon other conditions than the ones we tested in this study, for example, in response to nutrient limitation.

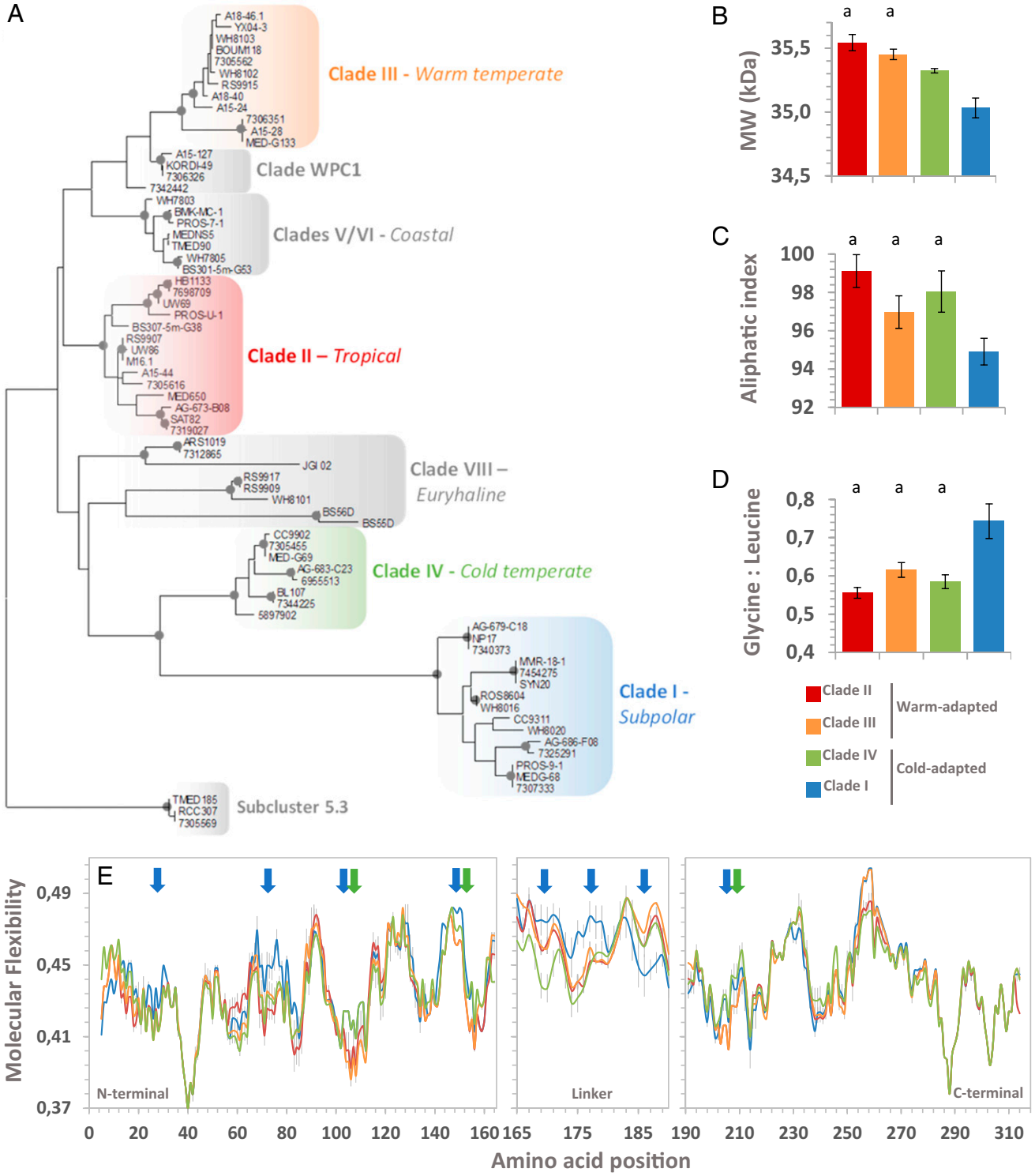

Fig. 4. Molecular characteristics of OCPs from marine *Synechococcus*. (*A*) On the left, the phylogenetic tree of OCP sequences collected in genomes and metagenomes, built using the maximum likelihood method (Jones–Taylor–Thornton model with gamma distribution, 500 bootstrap replications). The same tree configuration was obtained using the neighbor-joining method (Poisson model with gamma distribution, 2,000 bootstrap replications). Bootstrap values >85 are indicated on the nodes by a gray circle. The four dominant *Synechococcus* clades are shown in colors and the minor clades, whose thermophysiology has not been yet characterized, are shown in gray. On the right, clade average molecular characteristics of OCPs from marine *Synechococcus* OCPs tropical clade II (10 sequences, red), warm temperate clade III (10 sequences; orange), cold temperate clade IV (5 sequences, green), and subpolar clade I (13 sequences, blue), including the molecular weight (MW, *B*), the global aliphatic index reflecting the volume of aliphatic groups (*C*), the molar glycine to leucine ratio (*D*), and the predicted average flexibility along the amino acid sequence of the OCP linker region (*E*). Blue and green arrows show the region where clade I and clade IV display differences in predicted molecular flexibility. Statistics tests (Kruskal–Wallis test, $df = 3$ and P value < 0.05) are represented with the letter notation.

In order to validate our hypotheses, we studied the thermal niches and the prevalence of marine OCPs in natural *Synechococcus* communities by analyzing metagenomic surface samples of 42 stations of TARA expeditions (Fig. 5*A*). We recruited and enumerated the different marine *Synechococcus ocp* gene variants and plotted their relative percentages against in situ seawater temperature (Fig. 5*B*). Subpolar clade I *ocp* genes were present in the 6 to 22 °C range with maximal relative abundances at temperatures lower than 15 °C. Cold, temperate clade IV *ocp* genes were observed between 11 and 22 °C, with maximal values at ∼17 °C. Warm-adapted clades III and II *ocp* genes were present from temperatures higher than 15 °C. The relative abundance of warm, temperate clade III *ocp* genes was maximal between 17 and 25 °C at several Mediterranean stations in which clade III strains are known to dominate the *Synechococcus* communities (3, 11). The tropical clade II *ocp* genes accounted for more than 80% of the reads recruited when the seawater temperature was higher than 22 °C. These thermal distributions are in agreement with the definition of the in situ thermal niches of the four *Synechococcus* clades (3, 4, 6), as well as the thermal preferenda determined experimentally on representative laboratory strains (8, 9, 11).

We studied the prevalence of each of the four *ocp* variants by calculating the ratio of the abundance of *ocp* variants in the metagenomes to the corresponding abundance of the *petB* gene of the whole *Synechococcus* community (Fig. 5 *C*–*F* and *SI Appendix*, Table S3). As *petB*, encoding a subunit of the cytochrome b_6/f, is a core gene present in a single copy in all *Synechococcus* genomes; this ratio reflects the probability for a *Synechococcus* genome to possess a given *ocp* gene variant. Cold-adapted *ocp* genes (clades I and IV) showed similar thermal patterns of

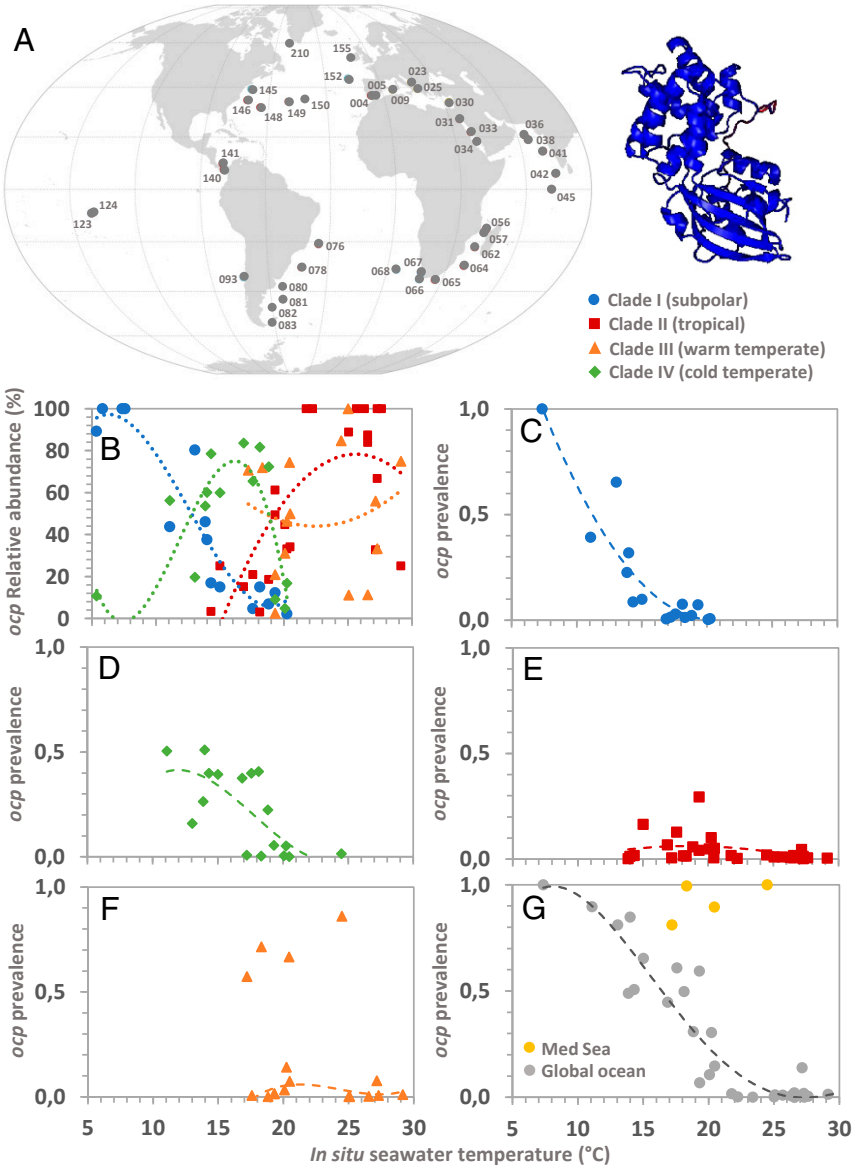

Fig. 5. Metagenomic analysis of the thermal distribution of *ocp* genes from marine *Synechococcus*. (*A*) Map showing the sampling stations of the TARA biosamples used in this study and a predicted structure model of marine OCPs (*SI Appendix*). (*B*) The relative abundance of the four dominant *ocp* gene variants, function of the seawater temperature, was expressed in percentages of the sum of the total abundance of these four genes. Values lower than 2% were excluded for better readability. The prevalence of the subpolar clade I (*C*), cold temperate clade IV (*D*), tropical clade II (*E*), and warm temperate clade III (*F*) *ocp* gene variants, function of sea water temperature, was calculated by dividing the normalized abundances of each *ocp* gene by the total abundance of the single-copy core gene *petB* of all *Synechococcus* clades. (*G*) The total *ocp* gene prevalence, including all known *Synechococcus* clades possessing the *ocp* gene, was calculated in the same way. Polar stations that exhibited too few reads were excluded from the analysis.

prevalence with maximal values in their respective (overlapping) thermal niches. In the warm-adapted *Synechococcus* clade II and III, the prevalence values of the *ocp* genes were much lower than in the cold-adapted *Synechococcus*. This was particularly noticeable for the tropical clade II *ocp* genes, which were often quasiabsent, even at stations where clade II *Synechococcus* are known to account for more than 90% of the whole *Synechococcus* community (3). This observation strongly supports the hypothesis that many tropical clade II *Synechococcus*, the most abundant *Synechococcus* cells in the world ocean, do not have the OCP operon. Studying in more detail the intraclade prevalence of the *ocp* gene variants (i.e., the number of *ocp* sequences divided by the number of *petB* sequences for a given clade) showed that clade II *Synechococcus* communities tend to have the *ocp* gene at the lowest temperature of the thermal distribution of this clade (<19 °C; *SI Appendix*, Fig. S16*E*).

A noticeable exception was observed for the warm, temperate clade III *Synechococcus* of the Mediterranean stations, in which the *ocp* prevalence was high. Therefore, in contrast to other regions of the world ocean, it seems that clade III *Synechococcus* inhabiting the Mediterranean Sea have retained the OCP operon during their evolution. Of note, this type of observation has already been reported regarding their membrane lipid metabolism (11). These genomic particularities could be interpreted as adaptive traits to the marked seasonality prevailing in the Mediterranean Sea. The OCP might indeed be useful in winter, during which the temperature can decrease down to ∼12 °C.

Finally, we recruited the *ocp* genes for the whole marine *Synechococcus* radiation and studied the global thermal prevalence of all *Synechococcus ocp* genes, including all the clades having the OCP operon (Figs. 4*A* and 6*G* and *SI Appendix*, Fig. S16). Excluding the Mediterranean Sea stations, the *Synechococcus ocp* prevalence in the world ocean showed a clear decreasing trend from the subpolar to the highest-seawater temperatures. At temperatures higher than 29 °C, the *ocp* gene was hardly detectable in any *Synechococcus* genome. Overall, our analysis strongly suggests that, among the *Synechococcus* lineages that have the OCP operon, the capacity to dissipate excess light as heat using the OCP is linked to the thermal niche. We also plotted the data against the seawater concentrations in nitrate, nitrite, ammonium, and iron. While none of these nutrients correlated with the *ocp* prevalence (*SI Appendix*, Fig. S17), suggesting that the presence of the *ocp* gene is not directly related to nutrient availability at global scale, additional observations in waters richer in nutrients could help clarify a possible role of nutrients in the capacity to dissipate excess light.

Metabolic Cost of Thermoacclimation in Marine *Synechococcus*. The thermophysiological strategies we unveil in this study imply the different costs of resource allocation to the photosynthetic apparatus. We retrieved from the genomes of M16-1 and MVIR-18-1 the sequences of the proteins constituting the phycobilisome, PSII, PSI, and OCP, and calculated the number of amino acids, carbon, nitrogen, and sulfur allocated to these pigmented protein complexes, taking into account the known stoichiometry of the protein subunits and bound chromophores (Dataset S1). Using our quantitative data and considering that a *Synechococcus* cell contains ∼300 fg/carbon (17, 52), we found that the pigmented protein complexes may represent up to 30 and 55% of the total carbon cell content in the clade I subpolar and clade II tropical strains we studied, respectively. This analysis revealed that, while the subpolar strain increased by 2.3-fold the cellular quota of amino acids, carbon, nitrogen, and sulfur allocated to pigmented protein complexes between 9 and 25 °C growth temperature, the thermal response of the tropical strain implied an ∼8.5-fold increase of this material between 17 and 31 °C growth temperature. Interestingly, when the data were converted from units per cell to biovolume units, the responses became linear, and we were able to determine that this corresponds to a temperature-induced increase in carbon biovolume content of 3.3 and 13.2 fg · C · μm^{-3} · $°C^{-1}$, for the subpolar and tropical *Synechococcus* strains over their growth thermal range, respectively (*SI Appendix*, Fig. S18). The capacity of clade II *Synechococcus* to rapidly allocate much of the resource to the photosynthetic apparatus may be interpreted as an opportunistic strategy that allows these cyanobacteria to efficiently benefit from the high temperatures that prevail in their ecological niche. In the context of a globally warming ocean, this can likely increase the competitiveness of tropical clade II *Synechococcus*, notably with respect to *Prochlorococcus* surface ecotypes, which grow more slowly (53). It is also worth noting that the high abundance of *Synechococcus* have been suggested to contribute to the long-term degradation of marine food webs in shelf waters (54).

Acclimation to higher temperatures required increasing sixfold the content in iron associated to the pigmented photosynthetic complexes, mostly due to PSI synthesis (Dataset S1). However, the cellular cost in photosynthetic iron for acclimating to high temperatures was similar between the two temperature ecotypes over their whole, thermal growth range. Both thermoacclimation responses were accompanied by a decrease in the C:N ratio of the pigmented protein complexes pool, which was twofold higher in *Synechococcus* sp. M16.1, indicating a higher-nitrogen cost for thermoacclimation of the photosynthetic apparatus in the tropical strain (Dataset S1). While the cost in carbon can be covered by a consequent increase in photosynthetic carbon fixation, this is not true for nitrogen. Marine *Synechococcus* are not diazotrophic cyanobacteria and, therefore, rely on the dissolved sources of nitrogen, which are present at very low concentration in oligotrophic waters. Thus, our analysis suggests that the physiological strategy used by tropical *Synechococcus* to rapidly and considerably increase their growth rate, with increasing temperature (Fig. 1*D*; 8), is probably efficient in mesotrophic areas, such as coastal waters, but might be unsuitable in oligotrophic niches. Although such analysis has never been carried out for *Prochlorococcus*, it is interesting in this context to recall that the latter picocyanobacterium has been able to colonize the warmest and most oligotrophic oceanic zones, evolving from the *Synechococcus* radiation, notably by considerably decreasing the metabolic cost of its photosynthetic antenna (55).

Conclusion

Phytoplankton drives the major part of the global carbon pumping of the world ocean through the photosynthesis process. This activity is highly influenced by temperature, which constrains most enzymatic reactions, such as those utilizing the photosynthetically produced ATP and NADPH molecules. The abundant and widespread marine *Synechococcus* have colonized different thermal niches through evolutionary specialization processes, leading to the differentiation of lineages adapted to different temperature ranges. Here, we show that the major *Synechococcus* lineages have considerably adapted their physiological strategies of light utilization to the constraints imposed by different temperature regimes. The tropical clade II *Synechococcus* are unable to grow at low temperature but, upon a temperature increase, they can rapidly develop very large capacities of light harvesting and utilization, which allow them to grow at impressive growth rates. By contrast, the *Synechococcus* adapted to subpolar niches can only moderately increase their efficiency of light utilization with increasing temperature but are able to cope with low temperatures by dissipating light that cannot be used in these conditions, thereby protecting the cell from oxidative stress. For this, they use the OCP, which has evolved differently in the different marine *Synechococcus* thermotypes. In the two phylogenetically distant cold-adapted lineages, it appears that an evolutionary convergence mechanism has adapted the OCP to cold niches by modifying the flexibility of the protein at certain crucial sites. By contrast, although some tropical *Synechococcus* might have gained the OCP operon through a more recent horizontal transfer, most of them

have lost the OCP operon during evolution, and when it is present, it provides the cell only moderate capacities of excess light dissipation, with regards to temperature variations. This shows that, in the oceans, temperature has been a major driver of the evolution of this important photosynthetic protein.

This study provides a prime example of the effects of the interaction of temperature with the light on the evolution of important marine primary producers. One key part of the evolutionary response has been the modulation of the tradeoff between light utilization and dissipation inducing, in marine *Synechococcus*, permanent modifications of the activity of the phycobilisomes (12) and the OCP in lineages that have colonized different thermal niches. We hypothesize that the opportunistic tropical clade II *Synechococcus* might become competitive phytoplankton in nitrogen-rich areas in the context of ocean warming, because they could considerably increase their efficiency of light utilization. The physiological strategies we have evidenced here can allow the improvement of the current hypotheses and models that aim at predicting the changes in carbon fluxes and food webs in the oceans in response to global warming.

Materials and Methods

Culture Conditions and Flow Cytometry. Clonal *Synechococcus* strains, including tropical (M16.1, RS9907, A15-44, and WH7803); warm, temperate (RS9915, WH8102, and BOUM118); cold, temperate (BL107 and MVIR-16-1); and subpolar (MVIR-18-1, SYN20, and WH8016) representatives, were retrieved from the Roscoff Culture Collection (*SI Appendix*, Table S1) and grown, as previously described (12), under continuous 80 μmol · photons · m^{-2} · s^{-1} white light supplied by multicolor light-emitting diode arrays. Cultures were long term acclimated from 9 to 35 °C within temperature-controlled chambers and maintained in the exponential growth phase.

Cell densities and fluorescence (excitation 488 nm, emission 525 ± 26 nm for PE, and 680 ± 30 nm for chl *a*) were measured on cultures preserved within 0.25% glutaraldehyde (Sigma-Aldrich) using a microplate flow cytometer (Guava EasyCyte HT). Growth rates were computed as the slope of a ln(Nt) versus time plot, where Nt is the cell concentration at time *t*. Biovolume measurements were carried out using a high-sensitivity cytometer (Novocyte Advanteon, Agilent) equipped with two lasers at 405 and 488 nm. The cell diameter *d* was estimated by measuring the forward light scatter of the *Synechococcus* population within a range of four sizes of silica beads.

In Vivo Fluorimetry. PAM measurements were carried out with a multiwavelength fluorimeter Phyto-PAM II (Walz), whose cuvette holder was maintained at growth temperature.

PSII quantum yield and fast kinetics. The PSII quantum yield F_V/F_M was measured, as previously described (8), for five wavelengths (440, 480, 540, 590, or 625 nm) of modulated light. To measure the PSII cross-section σ(II), dilute culture aliquots were incubated under weak far-red light inducing no significant PSII excitation and oxidizing the plastoquinone pool through PSI excitation. Single-turnover pulses were triggered to record O-I_1 fluorescence fast kinetics. Different pulse irradiances were tested to balance the photon dose function of the different wavelength absorption rates. The PSII cross-section $\sigma(II)_\lambda$ was calculated for each wavelength using the Phytowin 3 software [Walz; (56)].

PSII electron transport versus Irradiance curves. For each wavelength, after the measurement of the basal F_0 fluorescence level, twelve steps of 90 s increasing light irradiance were applied, with measurement of the instantaneous F_t and maximal F_M' fluorescence levels at the end of each step by triggering a multiple-turnover–saturating pulse. The PSII quantum yield under illuminated conditions was calculated as:

$$F_V'/F_M' = (F_M'-F_t)/F_M'.$$

The electron transport rate ETRII (e^- $PSII^{-1}$ s^{-1}) at PSII was calculated for each step according to the following (56):

$$\mathrm{ETRII} = \left(\left(F_V'/F_M'\right) \times \sigma(II)_{\lambda\,\mathrm{nm}} \times I \times 0.6022\right)/\left(F_V/F_M\right),$$

where I is the instantaneous irradiance at the considered step. ETRII values were plotted against instantaneous irradiance. The initial slope $\alpha_{(\lambda)}$, reflecting PSII efficiency under nonsaturating light, and the saturation irradiance $E_{K(\lambda)}$, where λ is the wavelength used for all light sources, were derived by fitting the photosynthesis Platt model (57).

Blue-green light–induced nonphotochemical quenching of fluorescence (NPQ_{BG}). Fluorescence traces were recorded using modulated light at 540 nm, predominantly absorbed by phycoerythrobilin-rich phycobilisomes. The culture sample was acclimated to 55 μmol · photons · m^{-2} · s^{-1} actinic blue-green light irradiance at 480 nm, then illuminated with 550 μmol · photons · m^{-2} · s^{-1} to measure possible NPQ_{BG} induction, and then brought back under low-light irradiance. During these sequences, F_M' was monitored by triggering saturating pulses. Actinic light was then turned off, and when the signal was down to the F_0 level, the F_M level was measured under 550 μmol · photons · m^{-2} · s^{-1} white light irradiance in the presence of 100 μM 3-(3,4-dichlorophenyl)-1,1-dimethylurea. When it occurred, NPQ_{BG} was expressed as the percentage of decrease of the maximal F_M' level. Light irradiance response curves for NPQ_{BG} were measured similarly, with 1-min steps of increasing 480 nm light irradiance.

Spectrofluorimetry. In vivo excitation spectra were recorded using a spectrofluorometer (PerkinElmer), as described in ref. 12.

High-Performance Liquid Chromatography. Volumes of 100 mL culture were harvested in presence of 0.01% pluronic (Sigma-Aldrich) by centrifugation at growth temperature (10,000 × *g*, 10 min) and stored at −80 °C until analysis. After extraction, in cold 90% methanol, the extracts were injected in an HPLC 1100 Series System (Hewlett-Packard) equipped with a C_8 column (Waters), as described in ref. 58. The pigment cell contents were calculated using the flow cytometry cell counts. The xanthophyll 3′-hydroxyechinenone was purified from a 5 L culture of the MVIR-18-1 strain grown at 10 °C. The standard solution was quantified (59), and a calibration curve was used to quantify 3′-hydroxyechinenone in the samples.

Quantification of Photosynthetic Proteins by Fluorescence and Immunoblotting Assays. Volumes of 400 mL culture were extracted according to a previously described procedure (60). Protein concentration was determined by measuring absorbance at 280 nm and 0.5 to 4 μg protein (depending on the strain and the protein) was loaded on 4 to 12% acrylamide gels, along with known quantities of standard proteins. β-PE was quantified by fluorescence in the electrophoresed gels using an LAS-4000 imager (GE Healthcare). PEII standard proteins were obtained as described in ref. 12. PsbD, PsaC, and RbCL were quantified on PVDF membranes following a standard quantitative immunoblotting method (60). After chemoluminescence imaging, target protein concentrations were determined by fitting the sample signal on protein standard (Agrisera).

In Silico Molecular Characterization of Marine Synechococcus OCPs. We used GeneBank, the Cyanorak information system, and TARA metagenomic datasets to compile a database of 70 OCP sequences of marine *Synechococcus* (*SI Appendix*, Table S2). Sequences were aligned using Bioedit 7.2.3 (61), and the maximum likelihood and neighbor-joining phylogenies were built using MEGA 10.1.8 (62). Amino acid frequencies and physicochemical parameters were computed using ProtParam Tools (63). The molecular flexibility was studied with ProtScale. The crystal structure of *Synechocystis* sp. PCC 6803 [PDB 3MG1; (64)] was used as a template to produce homology models of the OCP of the MVIR-18-1 and M16.1 strains using Phyre^2 (65) then superimposed using PyMOL version 1.7.4 to examine the structural differences.

Metagenomic Analysis of the Geographic Distribution of Marine OCPs. A selection of 42 sampling stations covering a wide variety of thermal niches were selected from the TARA metagenomic datasets [*SI Appendix*, Table S3, (66); http://www.taraoceans-dataportal.org/top/?execution=e2s1]. Temperature and localization data for each station were retrieved from PANGAEA (https://doi.pangaea.de/10.1594/PANGAEA.840718). Metagenomic read libraries corresponding to the surface layer and the size fraction 0.2 to 1.6 μm for TARA_004 to TARA_052 and 0.2 to 3 μm for the other stations were selected for a total of 59 paired libraries. A selection of 33 OCP genes, retrieved from publicly accessible genomes of marine *Synechococcus* (subclusters 5.1 and 5.3) and covering all the marine OCP clades known to date, and the corresponding *petB* genes were quantified in the selected TARA marine metagenomes using the Salmon (67) quantification tools with the option «–meta» selected. Raw read estimates were then normalized by the libraries and gene sizes before comparison.

Data Availability. All study data are included in the article and/or supporting information.

ACKNOWLEDGMENTS. This work was supported by the French National program Ecosphère Continentale et Côtière. We warmly thank Cécile Jauzein from the laboratory Dynamiques des Ecosystèmes Côtiers (Ifremer Brest) for giving access to its flow cytometer, as well as Justine Piterra for cell size microscope measurements and protein complex representations. We are grateful to the Roscoff Culture Collection for maintaining the *Synechococcus* strains used in this study. We also acknowledge the commitment of the Tara Oceans coordinators and consortium, the Tara schooner, and its captains and crew.

1. P. Flombaum *et al*., Present and future global distributions of the marine cyanobacteria *Prochlorococcus* and *Synechococcus*. *Proc. Natl. Acad. Sci. U.S.A.* **110**, 9824–9829 (2013).
2. S. Mazard, M. Ostrowski, F. Partensky, D. J. Scanlan, Multi-locus sequence analysis, taxonomic resolution and biogeography of marine *Synechococcus*. *Environ. Microbiol.* **14**, 372–386 (2012).
3. G. K. Farrant *et al*., Delineating ecologically significant taxonomic units from global patterns of marine picocyanobacteria. *Proc. Natl. Acad. Sci. U.S.A.* **113**, E3365–E3374 (2016).
4. J. A. Sohm *et al*., Co-occurring *Synechococcus* ecotypes occupy four major oceanic regimes defined by temperature, macronutrients and iron. *ISME J.* **10**, 333–345 (2016).
5. M. D. Lee *et al*., Marine *Synechococcus* isolates representing globally abundant genomic lineages demonstrate a unique evolutionary path of genome reduction without a decrease in GC content. *Environ. Microbiol.* **21**, 1677–1686 (2019).
6. A. G. Kent *et al*., Parallel phylogeography of *Prochlorococcus* and *Synechococcus*. *ISME J.* **13**, 430–441 (2019).
7. T. Grébert *et al*., Light color acclimation is a key process in the global ocean distribution of *Synechococcus cyanobacteria*. *Proc. Natl. Acad. Sci. U.S.A.* **115**, E2010–E2019 (2018).
8. J. Pittera *et al*., Connecting thermal physiology and latitudinal niche partitioning in marine *Synechococcus*. *ISME J.* **8**, 1221–1236 (2014).
9. D. Varkey *et al*., Effects of low temperature on tropical and temperate isolates of marine *Synechococcus*. *ISME J.* **10**, 1252–1263 (2016).
10. J. Pittera *et al*., Thermoacclimation and genome adaptation of the membrane lipidome in marine *Synechococcus*. *Environ. Microbiol.* **20**, 612–631 (2018).
11. S. Breton *et al*., Unveiling membrane thermoregulation strategies in marine picocyanobacteria. *New Phytol.* **225**, 2396–2410 (2020).
12. J. Pittera, F. Partensky, C. Six, Adaptive thermostability of light-harvesting complexes in marine picocyanobacteria. *ISME J.* **11**, 112–124 (2017).
13. L. J. Ong, A. N. Glazer, Phycoerythrins of marine unicellular cyanobacteria. I. Bilin types and locations and energy transfer pathways in *Synechococcus* spp. phycoerythrins. *J. Biol. Chem.* **266**, 9515–9527 (1991).
14. C. Six *et al*., Diversity and evolution of phycobilisomes in marine *Synechococcus* spp.: A comparative genomics study. *Genome Biol.* **8**, R259 (2007).
15. F. Humily *et al*., A gene island with two possible configurations is involved in chromatic acclimation in marine *Synechococcus*. *PLoS One* **8**, e84459 (2013).
16. S. Khorobrykh, V. Havurinne, H. Mattila, E. Tyystjärvi, Oxygen and ROS in photosynthesis. *Plants (Basel)* **9**, 91 (2020).
17. C. Six, J. C. Thomas, B. Brahamsha, Y. Lemoine, F. Partensky, Photophysiology of the marine cyanobacterium *Synechococcus* sp. WH8102, a new model organism. *Aquat. Microb. Ecol.* **35**, 17–29 (2004).
18. C. Six *et al*., Two novel phycoerythrin-associated linker proteins in the marine cyanobacterium *Synechococcus* sp. strain WH8102. *J. Bacteriol.* **187**, 1685–1694 (2005).
19. T. Kay Holt, D. W. Krogmann, A carotenoid-protein from cyanobacteria. *BBA - Bioenerg.* **637**, 408–414 (1981).
20. A. Wilson *et al*., A soluble carotenoid protein involved in phycobilisome-related energy dissipation in cyanobacteria. *Plant Cell* **18**, 992–1007 (2006).
21. F. Muzzopappa, D. Kirilovsky, Changing color for photoprotection: The orange carotenoid protein. *Trends Plant Sci.* **25**, 92–104 (2020).
22. D. Kirilovsky, Photoprotection in cyanobacteria: The orange carotenoid protein (OCP)-related non-photochemical-quenching mechanism. *Photosynth. Res.* **93**, 7–16 (2007).
23. C. A. Kerfeld, M. R. Melnicki, M. Sutter, M. A. Dominguez-Martin, Structure, function and evolution of the cyanobacterial orange carotenoid protein and its homologs. *New Phytol.* **215**, 937–951 (2017).
24. F. Muzzopappa, A. Wilson, D. Kirilovsky, Interdomain interactions reveal the molecular evolution of the orange carotenoid protein. *Nat. Plants* **5**, 1076–1086 (2019).
25. A. S. Palacio *et al*., Changes in population age-structure obscure the temperature-size rule in marine cyanobacteria. *Front. Microbiol.* **11**, 2059 (2020).
26. U. Schreiber, C. Klughammer, J. Kolbowski, High-end chlorophyll fluorescence analysis with the MULTI-COLOR-PAM. I. Various light qualities and their applications. *PAM Appl. Notes* **1**, 1–21 (2011).
27. A. P. Cavanagh, D. S. Kubien, Can phenotypic plasticity in Rubisco performance contribute to photosynthetic acclimation? *Photosynth. Res.* **119**, 203–214 (2014).
28. R. F. Sage, D. A. Way, D. S. Kubien, Rubisco, Rubisco activase, and global climate change. *J. Exp. Bot.* **59**, 1581–1595 (2008).
29. J. Galmés, I. Aranjuelo, H. Medrano, J. Flexas, Variation in Rubisco content and activity under variable climatic factors. *Photosynth. Res.* **117**, 73–90 (2013).
30. C. Liang, F. Zhao, W. Wei, Z. Wen, S. Qin, Carotenoid biosynthesis in cyanobacteria: Structural and evolutionary scenarios based on comparative genomics. *Int. J. Biol. Sci.* **2**, 197–207 (2006).
31. C. Boulay, A. Wilson, D. Kirilovsky, "Orange carotenoid protein (OCP) related NPQ in Synechocystis PCC 6803 OCP-phycobilisomes interactions" in *Photosynthesis. Energy from the Sun: 14th International Congress on Photosynthesis*, J. F. Allen, E. Gantt, J. H. Golbeck, B. Osmond, Eds. (Springer, 2008), pp. 997–1000.
32. M. Gwizdala, A. Wilson, D. Kirilovsky, In vitro reconstitution of the cyanobacterial photoprotective mechanism mediated by the orange carotenoid protein in *Synechocystis* PCC 6803. *Plant Cell* **23**, 2631–2643 (2011).
33. C. Boulay, L. Abasova, C. Six, I. Vass, D. Kirilovsky, Occurrence and function of the orange carotenoid protein in photoprotective mechanisms in various cyanobacteria. *Biochim. Biophys. Acta* **1777**, 1344–1354 (2008).
34. U. Guyet *et al*., Synergic effects of temperature and irradiance on the physiology of the marine *Synechococcus* strain WH7803. *Front. Microbiol.* **11**, 1707 (2020).
35. S. Takahashi, N. Murata, How do environmental stresses accelerate photoinhibition? *Trends Plant Sci.* **13**, 178–182 (2008).
36. H. Wu, S. Roy, M. Alami, B. R. Green, D. A. Campbell, Photosystem II photoinactivation, repair, and protection in marine centric diatoms. *Plant Physiol.* **160**, 464–476 (2012). Correction in: *Plant Physiol.* **160**, 1146 (2012).
37. H. Wu, A. M. Cockshutt, A. McCarthy, D. A. Campbell, Distinctive photosystem II photoinactivation and protein dynamics in marine diatoms. *Plant Physiol.* **156**, 2184–2195 (2011). Correction in: *Plant Physiol.* **176**, 960 (2018).
38. G. Ni *et al*., Arctic *Micromonas* uses protein pools and non-photochemical quenching to cope with temperature restrictions on photosystem II protein turnover. *Photosynth. Res.* **131**, 203–220 (2017). Correction in: *Photosynth. Res.* **136**, 127 (2018).
39. C. Djediat *et al*., Light stress in green and red Planktothrix strains: The orange carotenoid protein and its related photoprotective mechanism. *Biochim. Biophys. Acta Bioenerg.* **1861**, 148037 (2020).
40. A. Wilson *et al*., A photoactive carotenoid protein acting as light intensity sensor. *Proc. Natl. Acad. Sci. U.S.A.* **105**, 12075–12080 (2008).
41. H. Doré *et al*., Evolutionary mechanisms of long-term genome diversification associated with niche partitioning in marine picocyanobacteria. *Front. Microbiol.* **11**, 567431 (2020).
42. O. Ulloa *et al*., The cyanobacterium *Prochlorococcus* has divergent light-harvesting antennae and may have evolved in a low-oxygen ocean. *Proc. Natl. Acad. Sci. U.S.A.* **118**, e2025638118 (2021).
43. R. L. Leverenz *et al*., PHOTOSYNTHSIS. A 12 Å carotenoid translocation in a photoswitch associated with cyanobacterial photoprotection. *Science* **348**, 1463–1466 (2015).
44. B. W. Matthews, H. Nicholson, W. J. Becktel, Enhanced protein thermostability from site-directed mutations that decrease the entropy of unfolding. *Proc. Natl. Acad. Sci. U.S.A.* **84**, 6663–6667 (1987).
45. A. S. Panja, B. Bandopadhyay, S. Maiti, Protein thermostability is owing to their preferences to non-polar smaller volume amino acids, variations in residual physicochemical properties and more salt-bridges. *PLoS One* **10**, e0131495 (2015).
46. A. S. Panja, S. Maiti, B. Bandyopadhyay, Protein stability governed by its structural plasticity is inferred by physicochemical factors and salt bridges. *Sci. Rep.* **10**, 1822 (2020).
47. L. Garczarek *et al*., Cyanorak v2.1: A scalable information system dedicated to the visualization and expert curation of marine and brackish picocyanobacteria genomes. *Nucleic Acids Res.* **49**, D667–D676 (2021).
48. A. Fedida, D. Lindell, Two *Synechococcus* genes, two different effects on cyanophage infection. *Viruses* **9**, 136 (2017).
49. L. Huang *et al*., DprA is essential for natural competence in *Riemerella anatipestifer* and has a conserved evolutionary mechanism. *Front. Genet.* **10**, 429 (2019).
50. T. Hackl *et al*., Novel integrative elements and genomic plasticity in ocean ecosystems. *bioRxiv* [Preprint] (2020) https://www.biorxiv.org/content/10.1101/2020.12.28.424599v1. Accessed 15 March 2021.
51. A. Sedoud *et al*., The cyanobacterial photoactive orange carotenoid protein is an excellent singlet oxygen quencher. *Plant Cell* **26**, 1781–1791 (2014).
52. T. M. Kana, P. M. Glibert, Effect of irradiances up to 2000 $\mu E\ m^{-2}\ s^{-1}$ on marine *Synechococcus* WH7803-II. Photosynthetic responses and mechanisms. *Deep-Sea Res. A, Oceanogr. Res. Pap.* **34**, 497–516 (1987).
53. Z. I. Johnson *et al*., Niche partitioning among *Prochlorococcus* ecotypes along ocean-scale environmental gradients. *Science* **311**, 1737–1740 (2006).
54. K. Schmidt *et al*., Increasing picocyanobacteria success in shelf waters contributes to long-term food web degradation. *Glob. Change Biol.* **26**, 5574–5587 (2020).
55. C. S. Ting, G. Rocap, J. King, S. W. Chisholm, Cyanobacterial photosynthesis in the oceans: The origins and significance of divergent light-harvesting strategies. *Trends Microbiol.* **10**, 134–142 (2002).
56. U. Schreiber, C. Klughammer, J. Kolbowski, Assessment of wavelength-dependent parameters of photosynthetic electron transport with a new type of multi-color PAM chlorophyll fluorometer. *Photosynth. Res.* **113**, 127–144 (2012).
57. T. Platt, C. L. Gallegos, "Modelling primary production" in *Primary Productivity in the Sea*, P. G. Falkowski, Ed. (Springer, Boston, MA, 1980), pp. 339–362.
58. F. Partensky *et al*., A novel species of the marine cyanobacterium *Acaryochloris* with a unique pigment content and lifestyle. *Sci. Rep.* **8**, 9142 (2018).
59. S. Kosourov, G. Murukesan, J. Jokela, Y. Allahverdiyeva, Carotenoid biosynthesis in *Calothrix* sp. 336/3: Composition of carotenoids on full medium, during diazotrophic growth and after long-term H2 photoproduction. *Plant Cell Physiol.* **57**, 2269–2282 (2016).
60. F. Partensky *et al*., Comparison of photosynthetic performances of marine picocyanobacteria with different configurations of the oxygen-evolving complex. *Photosynth. Res.* **138**, 57–71 (2018).
61. T. A. Hall, BioEdit: A user-friendly biological sequence alignment editor and analysis program for Windows 95/98/NT. *Nucleic Acids Symp. Ser.* **41**, 95–98 (1999).
62. S. Kumar, G. Stecher, M. Li, C. Knyaz, K. Tamura, MEGA X: Molecular evolutionary genetics analysis across computing platforms. *Mol. Biol. Evol.* **35**, 1547–1549 (2018).
63. E. Gasteiger *et al*., "Protein identification and analysis tools on the ExPASy Server" in *The Proteomics Protocols Handbook*, J. M. Walker, Ed. (Humana Press, 2005), pp. 571–607.
64. A. Wilson *et al*., Structural determinants underlying photoprotection in the photoactive orange carotenoid protein of cyanobacteria. *J. Biol. Chem.* **285**, 18364–18375 (2010).
65. L. A. Kelley, S. Mezulis, C. M. Yates, M. N. Wass, M. J. Sternberg, The Phyre2 web portal for protein modeling, prediction and analysis. *Nat. Protoc.* **10**, 845–858 (2015).
66. S. Sunagawa *et al*., Structure and function of the global ocean microbiome. *Science* **348**, 1261359 (2015).
67. R. Patro, G. Duggal, M. I. Love, R. A. Irizarry, C. Kingsford, Salmon provides fast and bias-aware quantification of transcript expression. *Nat. Methods* **14**, 417–419 (2017).